Draft version November 3, 2021
Typeset using LaTeX **twocolumn** style in AASTeX631

Transit Hunt for Young and Maturing Exoplanets (THYME) VIII: a Pleiades-age association harboring a transiting planet detected by *Kepler*

Madyson G. Barber,[1] Andrew W. Mann,[1] Benjamin M. Tofflemire,[2,*] Jonathan L. Bush,[1] Adam L. Kraus,[2] Daniel Krolikowski,[2] Andrew Vanderburg,[2,†] Matthew J. Fields,[1] and Elisabeth R. Newton[3]

[1] *Department of Physics and Astronomy, The University of North Carolina at Chapel Hill, Chapel Hill, NC 27599, USA*
[2] *Department of Astronomy, The University of Texas at Austin, Austin, TX 78712, USA*
[3] *Department of Physics and Astronomy, Dartmouth College, Hanover, NH 03755, USA*

ABSTRACT

We describe a young association (MELANGE-2) in the *Kepler* field with a known planet candidate (KOI-3876.01) with signs of youth. To better determine the age and membership of MELANGE-2, we combine archival light curves, velocities, astrometry, with new high-resolution spectra of stars nearby KOI-3866.01 spatially and kinematically. The resulting rotation sequence, lithium levels, and color-magnitude diagram of members are all an excellent match for the Pleiades, confirming the population is co-eval and providing an age estimate of 110±10 Myr. KOI-3876's observed properties are an excellent match to the group, confirming membership. MELANGE-2 may be part of the larger Theia 316 stream, also estimated to be ≃108 Myr. For KOI-3876, we revise the stellar and planetary parameters of the system, taking into account the newly-determined age. We fit the 4.5 yr light curve from *Kepler* and find that KOI-3876.01 is a $2.0 \pm 0.1 R_\oplus$ planet that orbits its star every 19.58 days on an eccentric ($e > 0.2$) orbit. KOI-3876 was previously flagged as a likely eclipsing binary, but we rule this out using radial velocities from APOGEE and statistically validate the signal as planetary in origin based on archival follow-up and its *Kepler* light curve. Given its overlap with the *Kepler* field, we expect MELANGE-2 to be valuable for studies of spot evolution on timescales of years and KOI-3876 to be a piece of the growing work on transiting planets in young stellar associations.

Keywords: exoplanets, exoplanet evolution, young star clusters- moving clusters, planets and satellites: individual (KOI3876)

1. INTRODUCTION

Stellar clusters and associations serve as critical benchmarks for stellar and planetary astrophysics. Stars in such groups formed from the same interstellar cloud, and hence share a common (or similar) age, abundance pattern, and initial space velocity. The common set of properties makes it significantly easier to assign properties to the whole population, providing age estimates that are more precise and accurate than general-purpose techniques used outside clusters (e.g., Gyrochronology; **??**) and work on stars where ages are especially challenging (e.g., M dwarfs; **?**). Such coeval associations are therefore, ideal for how studying how stellar and planetary properties evolve with time (**??**).

Associations within the *Kepler* field have been especially valuable for stellar and planetary astrophysics. The ≃4.5 yr baseline and precise photometry enable precise measurements of rotation periods, even at older ages (e.g., **??**), providing some of the best constraints we have on the rotation evolution of stars past 1 Gyr (**??**). The four *Kepler* clusters (NGC 6866, NGC 6811, NGC 6819, and NGC 6791) have also provided a wealth of information about stellar mass-loss (**?**), post-main-sequence stellar evolution (**?**), and the occurrence of planets inside clusters (**?**).

The four known clusters in the *Kepler* field are all at distances of more than 1 kpc and ages ≳500 Myr. While these older ages (compared to nearby young groups) fill an important niche in stellar spin down and post-main-sequence evolution, their distance from the Sun

Corresponding author: Madyson G. Barber
madysonb@live.unc.edu

* 51 Pegasi b Fellow
† NASA Sagan Fellow

makes it challenging to study the low-mass members and search for small planets. The $K2$ mission covered many younger and more nearby clusters (**??**), but only for ≃80 days at a time. Searching for long-period planets and studying longer-term spot evolution with $K2$ data was therefore only possible in regions that $K2$ covered by multiple campaigns (**?**). Additional young associations in the *Kepler* field would provide the invaluable ≃4.5 yr baseline.

The availability of precise parallaxes and proper motions for millions of stars from *G*aia (**??**) has enabled the discovery of new coeval stellar associations (e.g., **??**). The `FriendFinder` code[1] (**?**) was designed to take advantage of *G*aia data, by searching for potential co-moving 'friends' around a user-identified young stars. This method has already been useful in finding the 250 Myr MELANGE-1 association (**?**) and age-dating a planet in the MOLUSC region of Lower-Centarus-Crux (Mann et al., any effing day now).

With the goal of finding previously undiscovered associations with transiting planets, we ran `FriendFinder` on *Kepler* objects of interest suspected to be younger than Hyades based on their lithium levels in **?**. The most promising association was a group of stars nearby KOI-3876, the candidate members of which showed a color-magnitude diagram consistent with the Pleiades. Here we describe our work demonstrating that this population is a real ≃ 110 Myr association (MELANGE-2) ≃300 pc from the Sun, as well as our validation of the KOI as a planet.

While the THYME survey was meant to focus on planets identified with *TESS*, KOI-3876 b was flagged as young by the same team and using the same methods as used extensively in the THYME and ZEIT series. Since the planet is not along the ecliptic, we opted to include it in the THYME survey series with a slight adjustment to the acronym.

The paper is organized as follows. In Section 2 we detail our initial selection of potential members of MELANGE-2. We list the range of archival and new data taken on candidate members of MELANGE-2 in Section 3. In Section 4 we demonstrate MELANGE-2 is a co-eval population and derive its overall properties and basic membership. Our effort to find known and new planets in MELANGE-2 is described in Section 5. We derive properties of the only identified planet in the association, KOI-3876 b, in Section 7, and statistically validate it in Section 7.1. We summarize our findings in Section 8 and briefly discuss the future utility of an association overlapping the *Kepler* field.

[1] https://github.com/adamkraus/Comove

2. TARGET SELECTION

As part of our effort to identify known planets in previously undiscovered young associations we ran the `FriendFinder` code (**?**) on all stars identified as young based on their lithium absorption (**?**); this initial seed list included KOI-3876. The `FriendFinder` algorithm uses *G*aia EDR3 positions, parallaxes, and proper motions to identify stars with similar Galactic tangential velocity and XYZ position to a selected input source. This required an absolute velocity for KOI-3876, for which we used the value from APOGEE (-26.79km s^{-1}, **?**).

The lithium levels suggested an age for KOI-3876 close to the Pleiades. Unbound or weakly bound associations >100 Myr should be significantly dispersed as they orbit through the Galaxy. So we used a generous selection, including any star within 5km s^{-1} and 50 pc of KOI-3876 as a candidate member. This yielded 1007 candidates.

We show the color-magnitude diagram (CMD) for our candidate members in Figure 1. The spread of the CMD suggests significant contamination; it is likely that most of the 1007 stars selected are not associated with KOI-3876. However, the CMD also shows there is significant contamination, there is also a sequence of the closest stars (in tangential velocity) consistent with the Pleiades single-star sequence. This matches the age suggested by the Li levels in KOI-3876.

3. OBSERVATIONS

3.1. *Optical spectra from McDonald 2.7 m Coudé*

We observed KOI-3876 and 21 association candidates (Section 2) with the Coudé spectrograph on the Harlan J. Smith 2.7m telescope at the McDonald Observatory. The Robert G. Tull Coudé is a cross-dispersed echelle spectrograph, delivering a R∼60,000 spectral resolution from 3400–10000 Å using the 1.″2 slit (**?**). Observations we're taken over the course of two observing runs, on 2021 July 9 and 2021 August 26–27. The sample was selected to include association candidates that could be observed with the Coudé in modest exposure times ($G < 13$), and spectral types later than mid-F ($B_p - R_P > 0.55$), where we expect lithium absorption to be a sensitive age diagnostic. The spectra are reduced with a custom python implementation of the standard IRAF procedures. Wavelength calibration made use of ThAr lamp spectra taken at the beginning, middle, and end of each night. the signal-to-noise of our spectra ranged between 14 and 60 per resolution element.

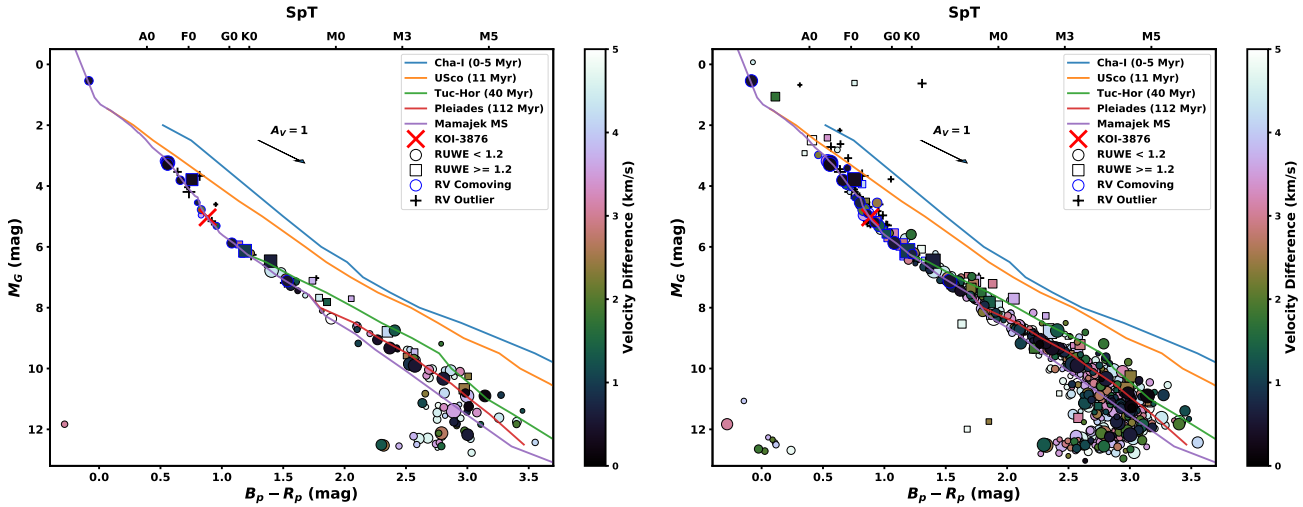

Figure 1. *G*aia color-magnitude diagram of all stars within 5 km s^{-1} in tangential velocity and 25 pc (left) or 50 pc (right) of KOI-3876. Points are color-coded by the difference between their expected and observed tangential velocity assuming a perfect *UVW* match to KOI-3876 and scaled in size by their distance from KOI-3876. Points with consistent radial velocities are given blue circles and those with discrepant velocities are plus signs (and are excluded from the color coding).

To assess whether association candidates are co-moving in three dimensions with KOI-3876, we measure radial velocities using spectral-line broadening functions (BFs). The BF is a linear inversion of an observed spectrum with a narrow-lined template, and represents the average stellar absorption-line profile. This profile (the BF) can be fit with a rotationally-broadened line profile to measure the stellar radial velocity and $v \sin i_*$. We compute BFs for 34 spectral orders between 4300 and 9800 Åthat are free of telluric contamination using the `saphires` python package (**?**). BFs from individual orders are combined in to a single, high SNR BF and fit with a rotationally broadened profile (**?**). Narrow-lined templates, specific to each star, are taken from the **?** PHOENIX model suite at the $T_{\rm eff}$ closest to that provided by the *TESS* Input Catalog (v8.0; **?**). Radial-velocity errors depend on the S/N and rotational broadening, but are generally on the order of 0.1 km s^{-1}. Measurements from the Coudé spectra are provided in Table **??**.

3.2. *Kepler Photometry*

To characterize the planet, KOI-3876 b, we obtained all *Kepler* photometry for KOI-3876. This included all Quarters (Q0-Q17), providing more than 4 years of long-cadence (30 m) photometry. To search for any additional planets in MELANGE-2, we also obtained *Kepler* photometry for any candidate member with a light curve, a total of 84 targets.

For both characterization and the search for additional planets we used the Pre-search Data Conditioning Simple Aperture Photometry (PDCSAP; **??**).

AWM: how many stars had TESS light curves (assuming they didn't have kepler curves? –MGB: 21 have both. Add to Kepler or Tess section? AWM: They need to know around how many stars we searched for planets out of the ¿1000 candidate stars. –MGB: end of Tess phot section

3.3. *TESS Photometry*

For candidate members of MELANGE-2 lacking *Kepler* data, we instead obtained *TESS* photometry to search for additional planet candidates. Again, we used PDCSAP flux, where available. This included a mix of 2-minute (9 targets) and 30-minute cadence data (47 targets), with 6 targets having both 2-minute and 30-minute cadence data.

Out of the original 998 friends identified, a total of 885 stars had neither *TESS* nor *Kepler*photometry, in most cases because they were too faint for the relevant survey. All light curves from *TESS*and *Kepler*were fed through //Notch and LOCoR// to look for additional transiting planets in the association. The process for the planet search, along with preliminary findings, is described in section 5.

3.4. *Archival photometry and astrometry*

We download positions, parallaxes, proper motions, and B_P, R_P and G photometry for all candidate members of MELANGE-2 using the third *G*aia Early Data Release (EDR3; **?**). For KOI-3876, we also retrieved photometry from the Two-Micron All-Sky Survey (2MASS; **?**), the Wide-field Infrared Survey Explorer (WISE; **?**), and the AAVSO All-Sky Photometric

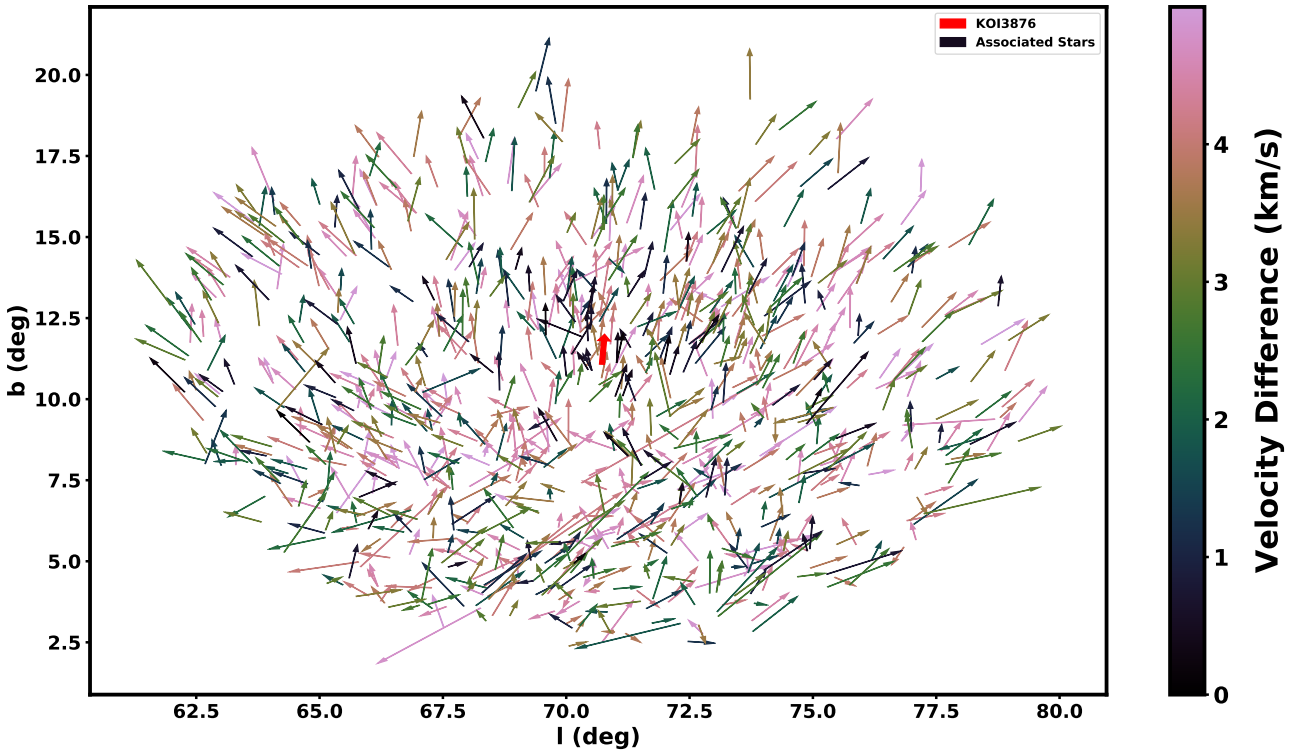

Figure 2. Here's an interesting caption.

Survey (APASS; **?**). Photometry for KOI-3876 is listed in Table 2.

3.5. *Archival Velocities*

In order of preference, we drew radial velocities for candidate MELANGE-2 members from the second *G*aia data release (DR2; **?**), the sixteenth APOGEE data release (DR16; **?**), and the fifth LAMOST data release (DR5; **??**). Velocities from our own spectra (Section 3.1) were given the highest priority. In the instance where a star had multiple velocities from the same star we used the weighted mean and error. We did not combine velocities from multiple sources due to possible differences in the zero-points.

In total, we adopted *G*aia RVs for 56 stars, APOGEE RVs for 5 stars, and LAMOST RVs for 25 stars. This was in addition to velocities from our Coude spectra for 22 candidate member stars as well as KOI-3876. We applied an offset to the LAMOST velocities of +4.54km s^{-1} based on the comparison from **?**. There may be additional zero-point differences between the velocity sources, but these are likely larger than the internal velocity spread within the group. The adopted velocities are given in Table **??**.

4. THE MELANGE-2 ASSOCIATION

4.1. *Position and Kinematics*

MGB: what goes here? ra/dec and velocity of the group?

We originally identified a group of 998 stars within 50pc and 5 km/s of KOI-3876using //friendfinder//.

As can be seen in Figure 3, most //give percentage// targets in the field have velocities greater than 4 km/s of KOI-3876, shown in pink. These are likely non-member background stars. However, we can see a cluster of high probability members that are within 1 km/s of KOI-3876, shown in black. We can see that these targets are tightly packed in z, between 58pc and 75pc, as expected based on the argument by //z argument paper//. In x and y, we see a streak as expected due to the rotation of the galaxy and the spreading of the cluster over time.

In Figure 2, we see a tight cluster of co-moving stars, shown in black surrounding KOI-3876, shown in red. We again see a large proportion of likely background stars moving separately from the core group.

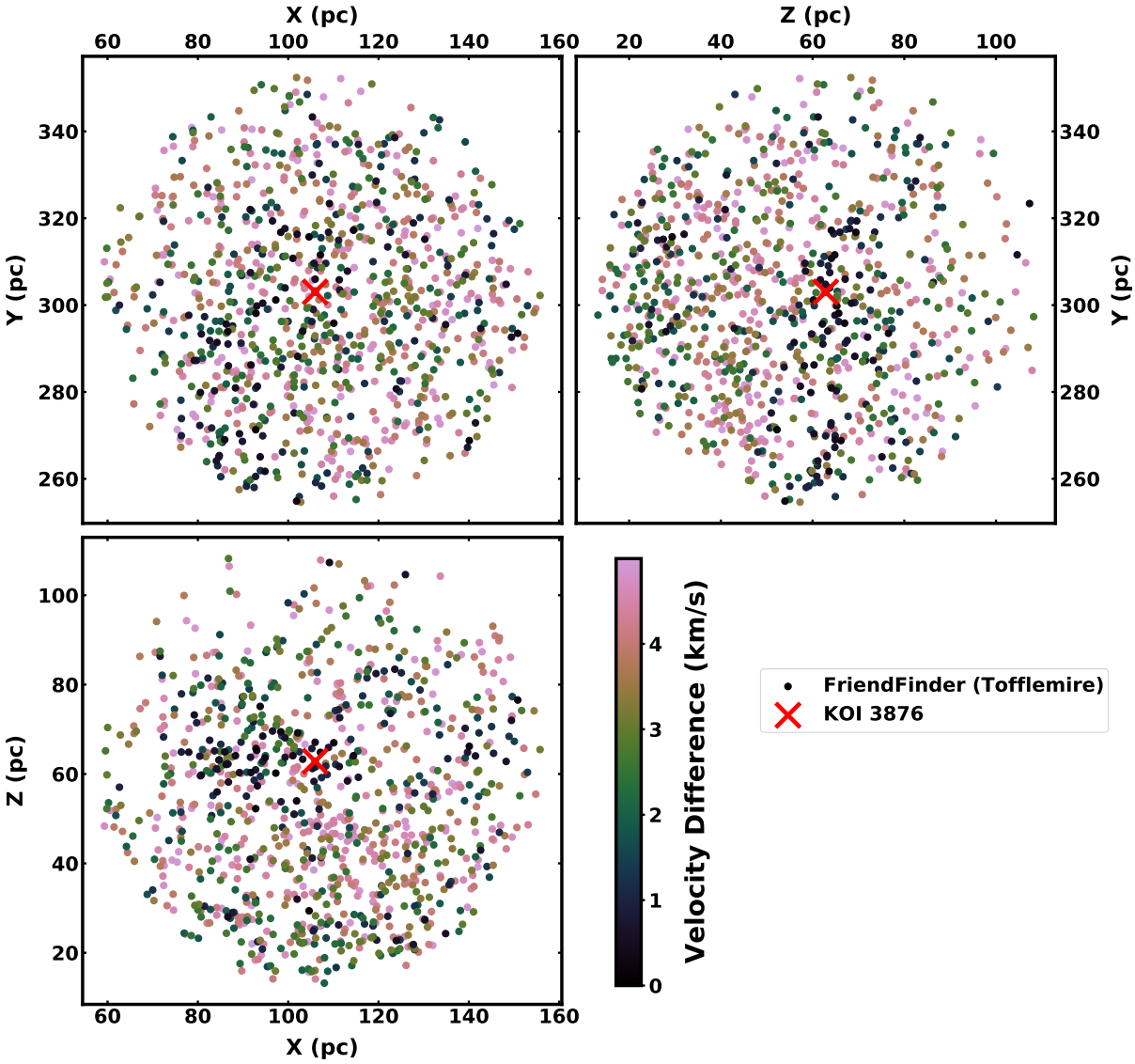

Figure 3.

4.2. *Isochronal age*

We estimated the age of MELANGE-2 by comparing the CMD to the PARSEC (v1.2S) models (**?**). We used a mixture model, as detailed in Mann et al. (in prep)[2], based on the method outlined in **?**, and wrapped in a Monte-Carlo Markov-Chain using `emcee` (**?**). To briefly summarize, we fit the population with the combination of two models. The first described the single-star member sequence drawn from PARSEC models. The second is an outlier population, which may contain a mix of populations (e.g., binaries, field interlopers, and stars with poor photometry or parallaxes). The fit included six free parameters: the association age (age), the average reddening across the association ($E(B-V)$), the amplitude of the outlier population (P_B), the mean offset from the CMD of the outliers (Y_B), the variance of the outliers around the mean (V_B), and a term to

[2] https://github.com/awmann/mixtureages

capture missing uncertainties or differential reddening across the association (f).

Reddening was limited to < 0.2 mag, based on the three-dimensional extinction map from **?**. Other parameters evolved under uniform priors, bounded only by physical limits. We re-sampled the model grid to ensure uniform distribution around the expected age (50-250 Myr).

*G*aia photometry was the only available for all targets, and was generally far more precise than other data available. Many stars were also resolved as binaries (or the target and a background star) in *G*aia, but seen as a single source in 2MASS and KIC photometry (**?**). So we restricted our analysis to *G*aia magnitudes. We also limited the membership list to those within 30 pc and 3km s^{-1} from KOI-3876 in three-dimensional distance and tangential velocity and removed any stars with a Renormalised Unit Weight Error (RUWE; **?**) > 1.2. As discussed in **?** and **?**, stars above this limit are likely to be binaries. Lastly, we removed any stars that were outside the model grid range based on their absolute magnitude and/or color. This left only 78 stars, but this was more than sufficient for a fit.

As we show in Figure 4, the resulting fit yields age of 104^{+8}_{-5} Myr. As a test of the systematic errors we ran a similar fit using models from the Dartmouth Stellar Evolution Program (DSEP, **?**) with magnetic enhancement from **?**. This yielded a similar age of 110±11 Myr. The DSEP magnetic models did somewhat better for the low-mass stars, and yielded a more conservative result, so we adopted this as the isochronal age.

4.3. *Lithium*

We measured the equivalent width of the Li 6708 Å line for 22 stars (including KOI-3876) using Coude spectra. With measured radial and rotation velocities from out BF analysis (Section 3.1), we shifted each spectrum to zero velocity and compared it to a rotationally broadened template of the same $T_{\rm eff}$. We then interactively define regions of continuum between 6685 and 6730 Å, and the bounds of the EW integration. We measured the Li EW and its uncertainty using a bootstrap approach. The continuum was first fit using `emcee`, 1000 random draws from the fit posterior are used to normalized the spectrum, and for each realization, the Li absorption line is numerically integration 10 times where the integration bounds are varied randomly from a normal distribution with the width of a resolution element. This procedure results in 10,000 Li EW measurements, we take the median and standard deviation as our final measurement and its uncertainty, respectively. We did not attempt to correct for contamination from the Fe

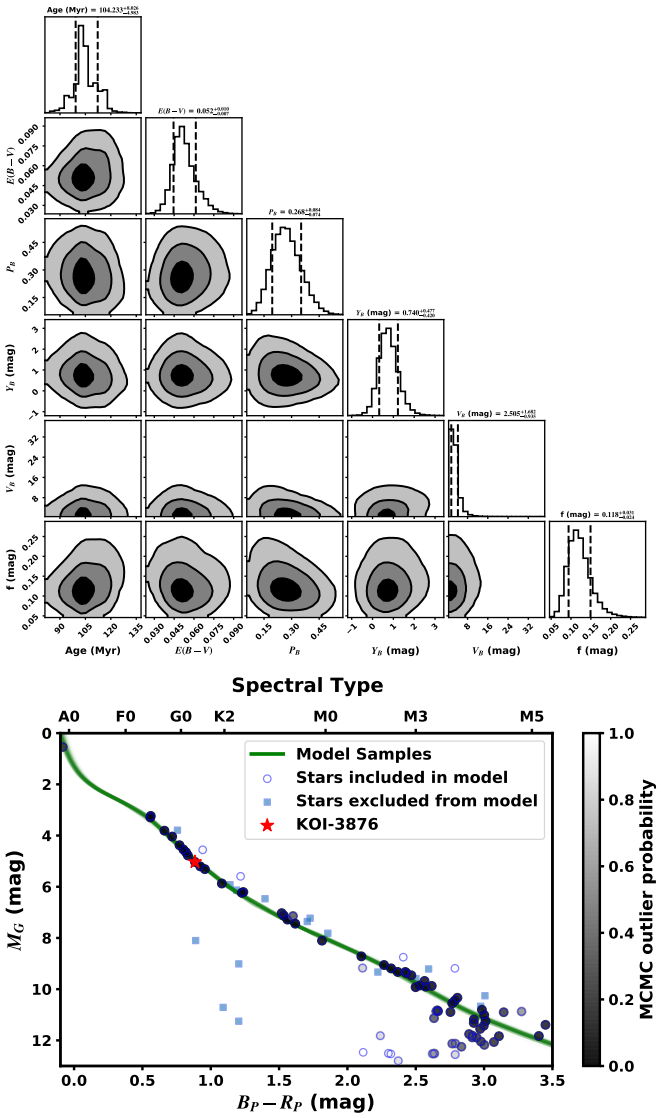

Figure 4. Comparison of the PARCSEC model isochrones to candidate members of MELANGE-2. The top shows the corner plot of our MCMC mixture model comparison, with contours corresponding to 1σ, 2σ, and 3σ. The bottom plot shows the *G*aia G versus $G - R_P$ CMD of stars included in the MCMC (blue circles) and those excluded (blue squares) due to their RUWE, color, or magnitude. Each included point is shaded based on their average outlier probability as determined by the MCMC. Many of those flagged as outliers may be non-members or members that do not follow the sequence (e.g., binaries). KOI-3876 is shown as a red star. The green lines are 200 PARSEC isochrones with parameters drawn (randomly) from the MCMC posterior.

line at 6707.44 Å or broad molecular contamination in the cooler stars, which likely set a limit on the precision of our equivalent widths at the ≃10% level.

Our sample included KOI-3876, for which we estimate a Li equivalent width if 134 mA. This is marginally

higher than (but consistent with) the value from **?** (120 mA). The larger value from our own analysis is likely because of different handling of the Fe line (10-15 ma). We used our measurement for consistency.

Two spectra (Gaia ID 2101333021814076800 and 2048317736525727488) had two clear sets of lines, indicating an SB2. For our Li measurements, we measured each line individually with a manually-applied offset. We then combined the two equivalent widths.

We compared the Li sequence for MELANGE-2 to that from the ≃112 Myr Pleiades **?** and the 650-700 Myr Hyades from (**?**) in Figure 5. The MELANGE-2 sequence is nearly identical to that from Pleiades

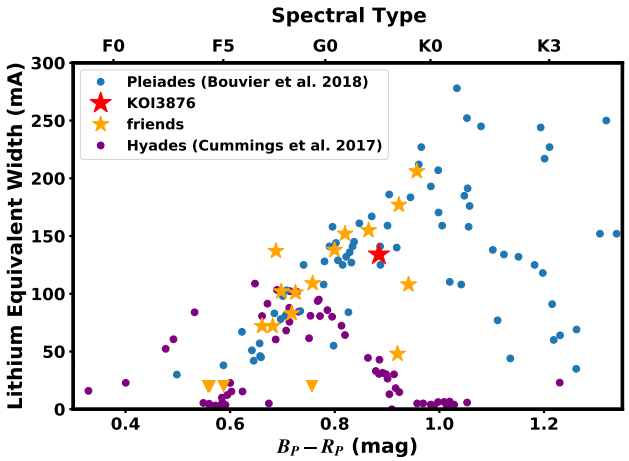

Figure 5. Lithium equivalent width as a function of *G*aia $B_P - R_P$ color for candidate members of KOI-3876 (MELANGE-2; orange), KOI-3876 (red), and members of the 125 Myr Pleiades from **?** and ≃700 Myr Hyades (**?**). We have excluded MELANGE-2 candidates with velocities inconsistent with membership. The MELANGE-2 sequence is consistent with Pleiades, other than 2 stars (which may be not members). The high levels of Lithium seen in the G dwarfs demonstrate the stars are much younger than Hyades.

4.4. *Rotation*

To better constrain the age of MELANGE-2 (and hence KOI-3876), we measured rotation periods for all candidate members using *Kepler* rotation measurements from the literature. as well as our own measurements from *Kepler*light curves and *TESS* full-frame images (FFIs).

First, candidate members were cross matched against Neilson //cite//, McQuillen 2013 and 2014 //cite//, and Santos 2019 and 2021 //cite// literature rotation periods. We identified 53 literature matches using the RA and DEC positions, except for when searching the Santos 2021 catalog, which we identified matches by KIC ID. McQuillen 2014 contained 52 matches, Neilson contained 37 matches, Santos 2019 contained 28 matches, Santos 2021 21 matches, and McQuillen 2013 6 matches. If multiple sources contained the target and the values agreed, the average rotation period was calculated. If the target was only available in one source, that value was used. Only one literature object, KIC 3743810, had disagreeing literature values. We examined the PDC-SAP light curve and selected the longer Nielsen rotation measurement.

Then, we downloaded *Kepler*PDCSAP light curves from the Mikulski Archive for Space Telescopes (MAST) for each candidate without a literature rotation. We searched the single-quarter light curves for rotation periods between $0.1 - 50$ days using the Lomb-Scargle algorithm (**?**) for each quarter of the 16 stars with available *Kepler*data. We selected the initial rotation from the quarter returning the rotation period with the highest Lomb-Scargle power. To confirm these measurements, we phase-folded the single-quarter light curves to the discovered period and examined the signals' consistency across quarters. We performed an eye-check in the style of **?**, labeling obvious rotations as Q0, questionable rotations as Q1, spurious detections as Q2, and non-detections as Q3. In total, 12 of the stars with Kepler data and no literature rotation returned usable rotations of quality Q0 or Q1.

For the rest of the candidates without rotations found in the literature or through our Kepler light curve measurements, we searched for *TESS*Full Frame Image data available through MAST. To generate the *TESS* light curves, we first created raw flux light curves from the FFI cutouts centered on each candidate. Then, we generated a Causal Pixel Model (CPM) of the telescope systematics using the `unpopular` package (**?**) for each individual star. We subtracted the CPM systematics from the initial light curves, resulting in the light curves used for our rotation search. After searching each single-sector light curve of each star for rotation periods from $0.1 - 30$ days using the Lomb-Scargle algorithm, we repeated the same rotation selection and quality check procedure as outlined for the Kepler data. We found 64 quality Q0 or Q1 rotations from the *TESS*CPM-subtracted light curves available.

In total we collected usable rotation periods (literature and Q0 or Q1) for 129 stars out of the 992 candidates, excluding KOI-3876. Of the 913 stars searched for in the TESS FFIs, 722 were too faint to retrieve a reliable light curve. Rotation period measurements from all sources discussed are included in Table **??**.

The rotation period distribution (Figure 6) is consistent with a Pleiades-age young association, except for

some Kepler field interlopers with rotations slower than the Pleiades sequence. Including the host star, 93 of out 130 stars with rotation measurements follow the Pleiades-age sequence.

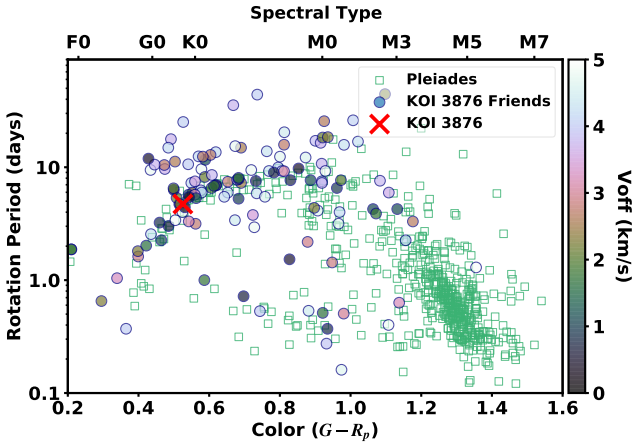

Figure 6. Rotation periods candidate members of MELANGE-2 (dark circles). Only literature measurements or stars with Q0 or Q1 rotations are shown. For reference, we show rotation periods from ≃110 Myr Pleiades (green squares; cite Rebull 2016 Multiperiod Pleiades stars).

5. SEARCH FOR PLANETS IN MELANGE-2

A number of known KOIs reside in the association. These targets and their planetary status can be found in Table 1.

We utilized Notch and LOCoR //cite// to look for planets in TESS and Kepler data. Notch and LOCoR are two methods of detrending the raw light curve to more easily see possible transits.

Notch attempts to fit a polynomial with a trapezoid (the "notch") to every point on the light curve. Notch detrends the light curve by flattening the polynomial that is used to model sections of the light curve. A Bayesian Information Criterion (BIC) value is assigned to every data point based on how well the notch models that point versus modeling the data point with just a polynomial without the trapezoidal cut out. The BIC takes into account the number of data points, the number of fit parameters, and the likelihood function of the model. The probability factor that we obtain is a measure of how well the model fits the data. These BIC values are normalized on a scale between 0 and 1, with 0 meaning the data point is very likely to be the center of a signal and 1 meaning there is likely no signal present at the data point.

LOCoR stands for Locally Optimized Combination of Rotations. The model is self-driven, meaning that the model will remove stellar variability based on the given stellar rotation period. Similarly to Notch, LOCoR detrends the light curve by using a polynomial model to flatten sections of the light curve.

The Box Least Squares (BLS) search in the Notch and LOCoR package uses the detrended light curve after running either Notch or LOCoR on the light curve. The function runs an iterative BLS search on either the detrended light curve or the BIC sequence of the light curve. It searches for transits by looking for regular small BIC values. If a planet is identified, it will be removed from the detrended light curve or BIC model before the algorithm looks for an additional planet.

We executed bulk searches of various stars in TESS data and Kepler data using Notch and LOCoR to look for promising targets. The THYME Team collaboration provided an initial list of known young stars from ESA's Gaia mission. Using the lightkurve python package //cite//, we obtained the light curve for each target and ran it through the Notch and LOCoR pipeline. We were able to identify the KOI3876 transit, as well as a number of other eclipsing binaries, KOIs, TOIs, and false positives in the association.

Using Notch and LOCoR, we identified 18 interesting targets. Eight of these are known KOIs (KOI-678.01, KOI-678.02, KOI-966.01, KOI-966.02, KOI-1838.01, KOI-5304.01, KOI-6819.01, and KOI-7059.01). KOI-1838.01, KOI-678.01, and KOI-678.02 are confirmed planets, while KOI-6819.01 is still considered a planetary candidate. Using existing spectra from Exofop (//cite//), radial velocities from Gaia (//cite//), and rotational periods and activity metrics where available, we conclude all KOIs except KOI-966 are likely not members of the association. Based on it's rotational period, KOI-966, a clear eclipsing binary, is still likely a member. Notch and LOCoR flagged KICs 1137886, 6134939, 6366739, 6589221, 9139566, and 9700914 and TICs 164461070, 20352534, 272486188, 273383615, 28768382, and 355909811 as interesting targets possibly containing one or more transiting bodies. Due to the low SNR, we just consider these candidates. We summarize all findings in Table 1.

5.1. *Discussion of individual candidates*

6. PARAMETERS OF THE PLANET HOST KOI-3876

We summarize constraints on the host star in Table 2, the details of which we provide in in this section.

6.1. *Literature Parameters*

As a reasonably bright (K_P = 12.6) star hosting a planet candidate from the *Kepler* mission, KOI-3876 has

Table 1. Planetary Candidates in MELANGE-2.

ID	Disposition	Probable Member?
KOI-678.01	Confirmed	N
KOI-678.02	Confirmed	N
KOI-966.01	EB	Y
KOI-966.02	EB	Y
KOI-1838.01	Confirmed	N
KOI-5304.01	FP	N
KOI-6819.01	Candidate	N
KOI-7059.01	EB	N
KIC 1137886	Candidate	
KIC 6134939	Candidate	
KIC 6366739	Candidate	
KIC 6589221	Candidate	
KIC 9139566	Candidate	
KIC 9700914	Candidate	
TIC 164461070	Candidate	
TIC 20352534	Candidate	
TIC 272486188	Candidate	
TIC 273383615	Candidate	
TIC 28768382	Candidate	
TIC 355909811	Candidate	

numerous stellar parameters in the literature. The California *Kepler* Survey estimate $T_{\rm eff}$=5720 ± 60 K, *log g* =4.64±0.1, and $v \sin i_*$=9.9±1.0km s^{-1}, $R_*0.95^{+0.06}_{-0.04} R_\odot$ and $M_* = 1.01 \pm 0.03 M_\odot$ based on comparing their high-resolution spectra and comparison to well-characterized templates (**??**) and stellar isochrones (**?**). **?**, using the same spectra, estimate $T_{\rm eff}$=5642±27 K, *log g* =4.46±0.05, $R_* = 0.93 \pm 0.02 M_\odot$, $M_* = 0.99 \pm 0.02 M_\odot$, and $v \sin i_*$=10.4±0.5km s^{-1}, as well as detailed abundances that are generally consistent with the Solar value. **?** incorporated *G*aia DR2 data with MIST stellar isochrones to derive an $T_{\rm eff}$=5577 ± 85 K, *log g* = 4.50 ± 0.02, and $R_* = 0.908 \pm 0.017 R_\odot$.

These stellar parameters are generally in agreement with each other. However, those that relied on isochrones (**???**) assigned > 1 Gyr ages, much older than the true ≃80 Myr age of KOI-3876. Although the assigned errors were large (and hence may be marginally consistent), the derived parameters may still be biased by the lack of an assigned age. Although this will not impact purely spectroscopic parameters like $T_{\rm eff}$ and $v \sin i_*$, the assumption can have a strong impact on the estimated stellar mass. Thus, we revisit these parameters with our own analysis below.

6.2. *Spectral-Energy Distribution*

.

We fit the observed spectral-energy-distribution (SED) following **?**. To briefly summarize, we fit the observed photometry with a grid of optical and near-infrared flux-calibrated spectra spanning 0.4–2.3μm. We included BT-SETTL CIFIST atmospheric models (**?**) in the fit, both to estimate the $T_{\rm eff}$ and fill in gaps in the template spectra (e.g., beyond 2.3μm). We integrated the resulting absolutely-calibrated spectrum to estimate the bolometric flux ($F_{\rm bol}$), which we combined with the *G*aia EDR3 parallax to estimate the stellar luminosity (L_*). With $T_{\rm eff}$ and L_*, we calculated R_* using the Stefan-Boltzmann relation. While reddening in this sight-line is low (**?**), KOI-3876 is well outside the Local Bubble, so we included extinction as part of the fit. To account for variability in the star, we added (in quadrature) 0.02 mags to the errors of all optical photometry. In total, the fit included six free parameters: the spectral template, A_V, three parameters that describe the model (log g, $T_{\rm eff}$, and [M/H]), and a scale factor between the model and the photometry. We show an example fit in Figure 7. The resulting fit yielded $A_V = 0.16^{+0.10}_{-0.08}$, $T_{\rm eff}$=5672 ± 65 K, $F_{\rm bol}$=(2.55 ± 0.10) × 10^{-10} (erg cm^{-2} s^{-1}), $L_* = 0.81 \pm 0.03 L_\odot$, and $R_* = 0.94 = 0.03 R_\odot$.

Our SED parameters were in good agreement with the literature spectroscopic values. Since the star is Sun-like, we considered the(high-resolution spectroscopic $T_{\rm eff}$ to be more reliable than the SED-based value, but the SED-based luminosity (and radius) more reliable than one derived from the spectroscopic *log g* or isochrone. We combined the two, which yielded a final radius of $0.92 \pm 0.02 R_\odot$.

6.3. *Isochronal parameters*

To determine M_* and verify our other stellar parameters, we compared the observed photometry to Solar-metallicity magnetic DSEP evolution models and PARSEC models. We used `emcee` to simultaneously fit for age, A_V, M_*, and an additional parameter to capture underestimated uncertainties in the data or models (f, in magnitudes) within an MCMC framework. We used a hybrid interpolation method, first identifying the nearest age in then model grid and then performing a linear interpolation in mass to obtain stellar parameters and model photometry. Since this method could not interpolate between ages, we re-sampled the input grid using the `isochrones` package (**?**) to be more dense (0.1 Myr and $0.01 M_\odot$) than expected errors. To redden the model photometry, we used `synphot` (**?**) and the extinction law from **?**. We placed a Gaussian prior on age of 110±11 Myr, while other parameters evolved under uniform priors. The resulting fit from each model grid was very precise, but differences between the two grids suggest larger systematic errors. Considering these,

Table 2. Properties of the host star KOI-3876.

Parameter	Value	Source
	Astrometry	
α	290.440629	*Gaia* EDR3
δ.	38.523572	*Gaia* EDR3
μ_α (mas yr^{-1})	-4.154±0.010	*Gaia* EDR3
μ_δ (mas yr^{-1})	2.269±0.011	*Gaia* EDR3
π (mas)	3.0565±0.0093	*Gaia* EDR3
	Photometry	
G_{Gaia} (mag)	12.6054±0.0028	*Gaia* EDR3
BP_{Gaia} (mag)	12.9642±0.0033	*Gaia* EDR3
RP_{Gaia} (mag)	12.0798±0.0041	*Gaia* EDR3
B (mag)	13.375 ± 0.094	APASS
V (mag)	12.655 ± 0.122	APASS
g' (mag)	13.038 ± 0.033	APASS
r' (mag)	12.456 ± 0.092	APASS
i' (mag)	12.323 ± 0.062	APASS
J (mag)	11.456 ± 0.02	2MASS
H (mag)	11.152 ± 0.016	2MASS
K_S (mag)	11.107 ± 0.019	2MASS
$W1$ (mag)	11.06 ± 0.023	ALLWISE
$W2$ (mag)	11.09 ± 0.020	ALLWISE
$W3$ (mag)	10.91 ± 0.094	ALLWISE
	Kinematics & Position	
RV$_{\rm Bary}$ (km s^{-1})	-26.79±0.01	?
	Physical Properties	
$P_{\rm rot}$ (days)	4.69 ± 0.04	McQuillan(?)
$v \sin i_*$(km s^{-1})	10.4 ± 0.5	?
$F_{\rm bol}$ (erg cm^{-2} s^{-1})	(2.55 ± 0.10) × 10^{-10}	This work
$T_{\rm eff}$ (K)	5720 ± 60	This work, CKS
[Fe/H]	0.12 ± 0.02	?
M$_\star$ (M$_\odot$)	1.01 ± 0.03	This work
R$_\star$ (R$_\odot$)	0.92 ± 0.02	This work
L$_\star$ (L$_\odot$)	0.81 ± 0.03	This work
$\rho_\star$ ($\rho_\odot$)	1.30 ± 0.10	This work
Age (Myr)	110 ± 11	This work

the resulting parameters were generally in agreement with our spectroscopic constraints ($R_* = 0.968 \pm 0.07$, $A_V = 0.27 \pm 0.10$, $T_{\rm eff}$=5710±60) and provided a stellar mass estimate of $M_* = 1.04 \pm 0.03 M_\odot$. We combined this with our earlier radius estimate to get an estimate of the stellar density ($\rho_* = 1.30 \pm 0.10 \rho_o dot$).

7. PARAMETERS OF KOI-3876 b

We fit the *Kepler* photometry using the `misttborn` (MCMC Interface for Synthesis of Transits, Tomography, Binaries, and Others of a Relevant Nature) fitting code[3] first described in ? and expanded upon in ?. `misttborn` uses `BATMAN` (?) to generate model light curves and `emcee` (?) to explore the transit parameter space.

[3] https://github.com/captain-exoplanet/misttborn

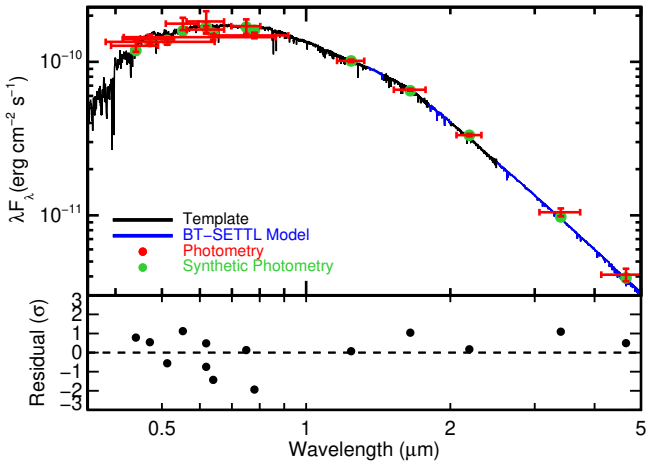

Figure 7. Best-fit template spectrum (G1V; black) and synthetic photometry (green) compared to the observed photometry of KOI-3876 (red). Errors on observed photometry are shown as vertical error bars, while horizontal error bars indicate the approximate width of the filter. BT-SETTL models (blue) were used to fill in regions of high telluric absorption or beyond the template range. The bottom panel shows the photometric residual in units of standard deviations.

The standard implementation of `misttborn` fits for six parameters for each transiting planet: time of periastron (T_0), orbital period of the planet (P), planet-to-star radius ratio ($R_p/R_\star$), impact parameter (b), and stellar density ($\rho_\star$). For each wavelength observed, we fit two linear and quadratic limb-darkening coefficients (q_1, q_2) following the triangular sampling prescription of ?. To cover all four bands (*TESS* and SDSS *griz*) required ten limb-darkening parameters in total. Gas drag and gravitational interactions are expected to dampen out eccentricities and inclinations of extremely young planets like KOI-3876 b (?), so we locked the eccentricity at zero.

We ran two versions of the fit. In the first, the MCMC chain restricted e to 0 and allowed $\rho_\star$ to vary within a uniform distribution, and the second allowed e to vary. In both fits, we ran the MCMC using 50 walkers for 250000 steps including a burn-in of 20000 steps. The autocorrelation times for both fits indicated that this was sufficient for convergence. We applied Gaussian priors on the limb-darkening coefficients based on the values derived using our stellar parameters from Section 6 and the `LDTK` toolkit ?, with errors accounting for the difference between models (0.42±0.08 and 0.13±0.04 for linear and quadratic, respectively). All other parameters were sampled uniformly with physically motivated boundaries: T_0 was restricted to the time period sampled by the data and $|b| < 1 + R_P/R_*$.

To model stellar variations, `misttborn` includes a Gaussian Process (GP) regression module, utilizing the `celerite` code (**?**). We used a mixture of two stochastically driven damped simple harmonic oscillators (SHOs) at periods P_{GP} (primary) and $0.5P_{GP}$ (secondary). In total, there were five GP parameters: the log of the dominant period ($\ln(P_{GP})$), the log of the GP amplitude ($\ln$ Amp), a decay timescale for the variability (quality factor, $\ln Q0$), the difference between the primary and secondary quality factors ($\ln \Delta Q$), and a mix parameter that describes how the primary and secondary signals are combined (Mix).

As we show in Figures 8, the SHOs GP did an excellent job describing the overall variability, even in the presence of complex changes in the light curve morphology. We also show the phase folded light curve in Figure 9 for the eccentric fit. The best-fit parameters with uncertainties for both fits can be found in Table 3, and the corner plot for the major transit-fit parameters for the eccentric fit is in Figure 10.

Based on the large $\rho_\star$ value for the fit where the eccentricity of the orbit was restricted to 0, we concluded the planet likely has an eccentric orbit. For a circular orbit, we expect the MCMC fitted $\rho_\star$ value to closely match the isochronal $\rho_\star$ value (as seen in Table 2). However, we find that these values match when the eccentricity of the orbit is non-zero. We favor the fit in which the eccentricity is allowed to vary.

7.1. *False Positive Analysis*

In **?**, the authors run the false-positive probability calculator `VESPA` **?** on all *Kepler* objects of interest, including KOI-3876 b. `VESPA` describe vespa. From this analysis, **?** assign a high probability (90%) that KOI-3876 b is an eclipsing binary, and $< 1\%$ that the signal is due to a planet overall. However, our light curve analysis reveals the expected U-shape transit for a planet, and there is no sign of a companion in the extant spectroscopy or adaptive optics imaging. It is possible the high **?** was an artifact of poor detrending of the high stellar variability in KOI-3876, motivating a re-analysis with a flattened light curve.

AWM: do we want to say something about the AO imaging somewhere. VESPA

8. SUMMARY AND CONCLUSIONS

KOI-3876 bis a // =// 110 Myr planet in the newly identified MELANGE-2association. KOI-3876 bis about twice the size of the earth, orbiting a star that is a young analog to the Sun, having a similar radius and mass. Originally flagged as a false positive by //false positive work//, we rule out this disposition based on APOGEE radial velocities and our own light curve analysis.

We used rotation periods, lithium, and isochronal evolution models in order to age MELANGE-2, and thus KOI-3876 b, to 110 ± 10 Myr.

Using misttborn, we find that KOI-3876 blikely has an eccentric orbit. We find that we can only match the fitted stellar density and the estimated isochronal density by allowing the eccentricity to vary in the fit rather than fixing it to 0. Because of this, we prefer the eccentric fit parameters over the fixed eccentricity fit.

Further, we identified additional candidates in the association for future follow-up that have potential of being planetary candidates.

ERROR: In AASTeX v6.3.1 the `\acknowledgments` command has been deprecated.
Instead, please use the begin/end form:
`\begin{acknowledgments}...\end{acknowledgments}`
when using acknowledgments. For more details, see:
https://journals.aas.org/aastexguide/#acknowledgments

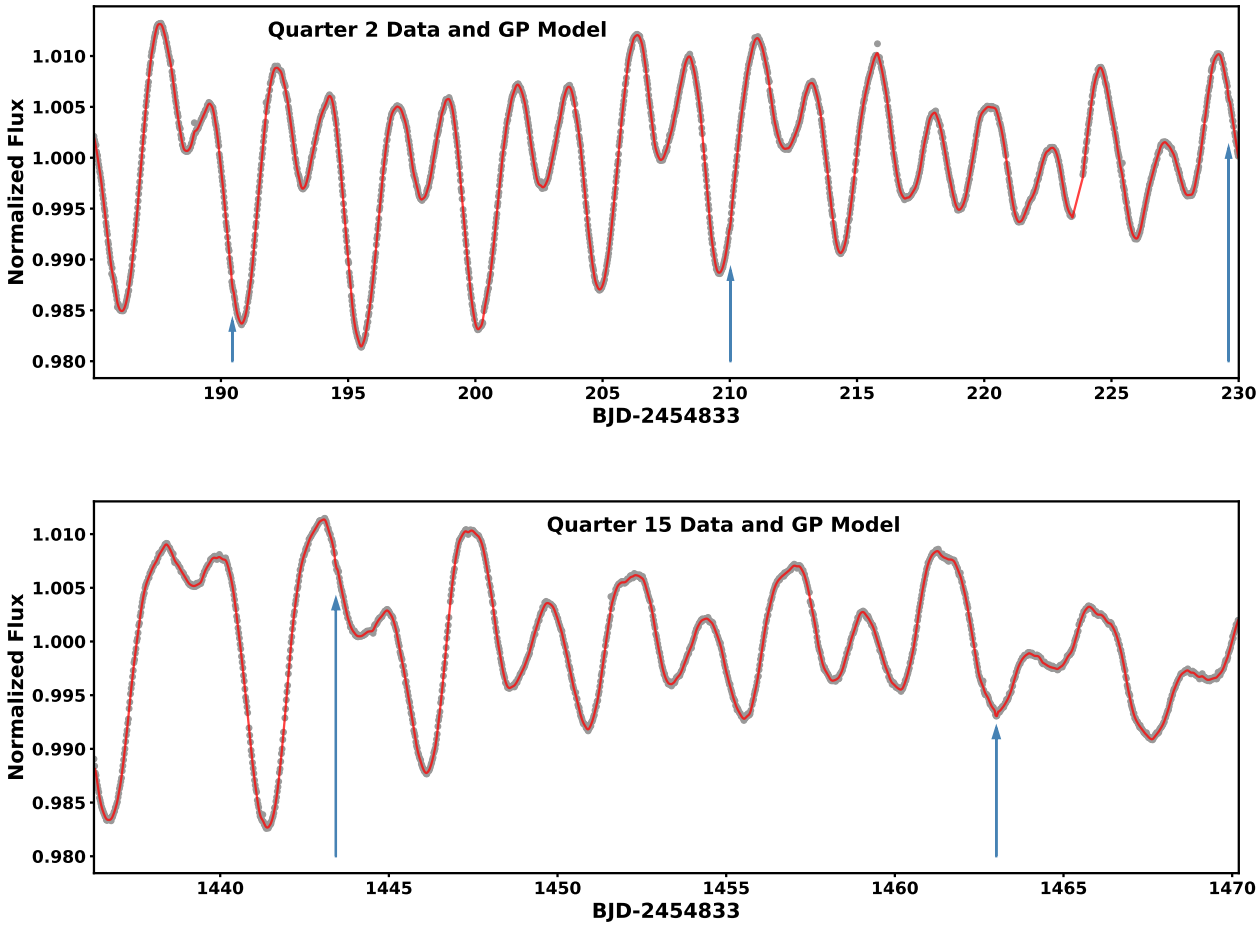

Figure 8. Approximately 40-day windows from *Kepler* Quarter 2 (top) and *Kepler* Quarter 15 (bottom) light curve of KOI-3876. The normalized flux (grey) is shown with our best-fit GP model (red). The locations of transits are shown with the blue arrows.

Table 3. Parameters of KOI-3876

Parameter	Value (e = 0)	Value (e varies)
Measured Parameters		
T_0 (BJD)	131.71494 ± 0.00087	$131.71488^{+0.00089}_{-0.0009}$
P (days)	$19.577829 \pm 2.1 \times 10^{-5}$	$19.57783^{+2.2\times10^{-5}}_{-2.3\times10^{-5}}$
$R_P/R_\star$	$0.01946^{+0.00061}_{-0.00043}$	$0.02112^{+0.00092}_{-0.00079}$
b	$0.31^{+0.28}_{-0.22}$	$0.803^{+0.081}_{-0.1}$
$\rho_\star$ ($\rho_\odot$)	$15.5^{+2.5}_{-5.9}$	$1.308^{+0.09}_{-0.089}$
$q_{1,1}$	$0.291^{+0.107}_{-0.099}$	$0.305^{+0.101}_{-0.096}$
$q_{2,1}$	$0.371^{+0.075}_{-0.086}$	$0.373^{+0.077}_{-0.09}$
$\sqrt{e}\sin\omega$	–	$0.29^{+0.16}_{-0.22}$
$\sqrt{e}\cos\omega$	–	-0.07 ± 0.48
$\log(P_{GP})$	1.5658 ± 0.0036	$2.09^{+0.012}_{-0.5}$
$\log(Amp)$	$-9.48^{+0.13}_{-0.12}$	$-9.348^{+0.095}_{-0.2}$
$\log(\Delta Q)$	2.41 ± 0.22	$108.7^{+170.0}_{-110.0}$
$\log(Q0)$	$1.36^{+0.059}_{-0.056}$	$1.195^{+0.162}_{-0.08}$
$\log(Mix)$	$-1.56^{+0.16}_{-0.17}$	$3.6^{+4.2}_{-5.1}$
Derived Parameters		
$a/R_\star$	$76.2^{+3.9}_{-10.0}$	$40.2^{+4.1}_{-4.4}$
i (°)	$89.76^{+0.17}_{-0.29}$	$88.56^{+0.19}_{-0.13}$
T_{14} (days)	$0.0794^{+0.0016}_{-0.0015}$	$0.097^{+0.044}_{-0.019}$
T_{23} (days)	$0.0756^{+0.0015}_{-0.0016}$	$0.085^{+0.042}_{-0.02}$
a (AU)	$0.326^{+0.018}_{-0.049}$	0.165 ± 0.029
e	–	$0.27^{+0.16}_{-0.14}$
ω (°)	–	$114.0^{+55.0}_{-73.0}$

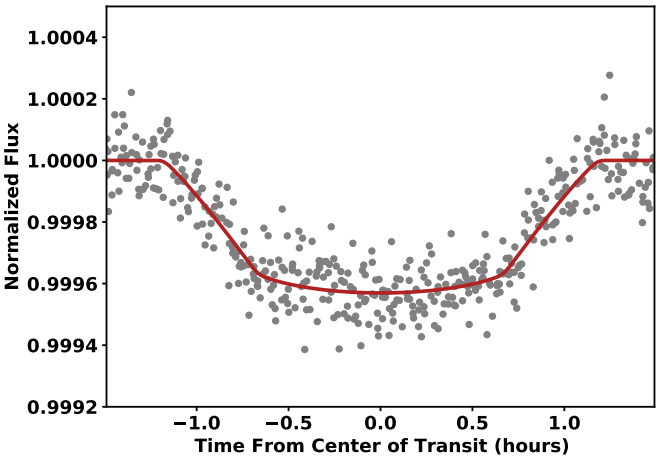

Figure 9. Phase-folded light curve of KOI-3876 (grey) with the best-fit transit model (red) using the eccentric fit. The best-fit GP model to the stellar variability has been removed.

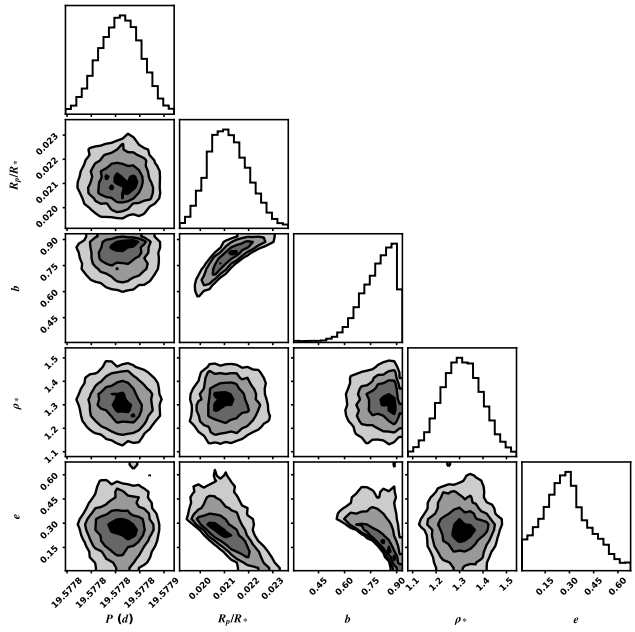

Figure 10. Corner plot?